Kinetics of Vacancy Doping in SrTiO₃ Studied by *in situ* Electrical Resistivity

Felipe Souza Oliveira[a] [●], *Ana Carolina Favero[a], Sergio Tuan Renosto[a], Mário Sérgio da Luz[a,b],*

Carlos Alberto Moreira dos Santos[a]

[a]*Escola de Engenharia de Lorena, Universidade de São Paulo, 12602-810, Lorena, SP, Brasil*
[b]*Instituto de Ciências Tecnológicas e Exatas, Universidade Federal do Triângulo Mineiro, 38025-180, Uberaba, MG, Brasil*

The kinetics of annealing to transform stoichiometric SrTiO₃ insulator into a vacancy-doped semiconductor-superconductor was revisited by *in situ* electrical resistivity measurements. SrTiO₃ single crystals were grown by Floating Zone Method. Using a homemade apparatus several electrical resistivity as a function of time were measured at different temperatures, which allows one to study the creation of vacancies during annealing under vacuum. The activation energy for the oxygen vacancies formation/charge doping in SrTiO₃ was estimated as 1.4±0.3 eV using solid-state kinetics approach.

Keywords: *strontium titanate, crystal growth, solid-state kinetics.*

1. Introduction

Strontium titanate (SrTiO₃) is one of the most studied cubic perovskites due to the fascinating physical properties[1-4]. This compound exhibits structural cubic to tetragonal transition at 105 K with a ferroelectric order simultaneous to antiferrodistorsive transition order[5]. The interplay between these distortions has been focus of many studies[6-8].

During last five decades, much attention has been given to the electronic transport mechanisms in doped SrTiO₃. This is special due to the anomalous superconductivity within a limited doping window[9-11] in the vicinity of a ferroelectric transition[12].

Stoichiometric SrTiO₃ is an insulator with 3.2 eV band gap, but one can introduce electron donor states by replacing Ti⁴⁺ by Nb⁺⁵[13] or Sr²⁺ by La³⁺ like a *n*-type silicon based semiconductor[14] either oxygen can be removed with heat treatment in vacuum at high temperatures in order to reach SrTiO₃₋δ vacancy self-doped semiconductors[15]. It is known that oxygen vacancies remain double ionized in quenched samples after annealing under vacuum, therefore, two free-electrons became available for each oxygen removed from the crystal lattice after the reduction process[16].

Several authors have studied the vacancy doping of SrTiO₃ in form of single crystals, thin films or ceramics[17-20]. Some of these authors have shown chemical diffusion coefficients for the SrTiO₃ crystal lattice using the Neumann solution of the Fick's second law carried out by *in situ* transient electrical resistivity measurements[18-20]. Additionally, in this paper we report that the solid-state kinetic models reviewed by Khawam and Flanagan[21] can describe the *in situ* electrical resistivity measurements as a function of time, which allows us to determine the energy involved in oxygen removal process from the SrTiO₃.

Thus, this paper deals with the SrTiO₃ single crystals grown by Floating Zone Method[22]. The reported data show that the self-doping in SrTiO₃₋δ is well described by a first order mechanism with an activation energy of 1.4±0.3 eV to produce oxygen vacancies, which is comparable to the recent data available on literature[23].

2. Experimental Procedures

2.1 Crystal growth and samples quality

Polycrystalline SrTiO₃ phase was synthetized from mixed SrCO₃ and TiO₂ powders with 99.9% purity (*Sigma-Aldrich* reagents). Precursor powders were mixed in liquid acetone under magnetic stirring. The resultant mixture was dried and then calcined in air at 1200°C for 24 hours. X-ray powder diffractometry technique with CuKα radiation and Ni filter using *PanAnalytical Empirian* diffractometer was employed to verify the phases present in the samples. Due to the heavier mass, the impurities have lower diffusion compared to oxygen atoms. Therefore, in this work we suppose that the sample impurities contents do not chance during the heat treatment and are not responsible for the electrical resistance change.

In order to grow single crystals of $SrTiO_3$ using the Floating Zone Method[22], polycrystalline powder was sealed in cylindrical rubbers and hydrostatically compressed into rods with 5 to 6 mm in diameter and 70 to 130 mm in length. The polycrystalline feed rods were sintered in air at 1300ºC for 12 hours in which 80 to 90% of theoretical density was obtained.

Floating Zone Method consists in directional solidification of a polycrystalline feed rod casted by concentrated radiation emitted from bulb lamps at the focus of concave ellipsoid mirrors. The desired single crystal grows by controlled solidifying of molten above the single crystal used as a seed while both are pulling downward from heating zone[24]. Our single crystals were grown at normal atmosphere using 8 mm/h growth rate, 35 rpm in clockwise, and 5 rpm in counterclockwise rotations for feed rod and seed. The *Quantum Design* Infrared Image Furnace used here has two bulb lamps with 650 W maximum power in each concave mirrors, one facing another. At least, 95% of the power lamp was required to achieve 2040ºC in order to melt the $SrTiO_3$ rods[25].

Obtained $SrTiO_3$ single crystals are transparent with light yellow color or brown color. It is well known that oxygen content and stoichiometry deviations can affect the color of single crystals[26]. In in this sense, eventual evaporations during crystal growth should explain the differences observed in the coloration of samples produced here.

After the growing, circular wafers were cut from single crystal bars with an *IsoMet* cutting machine. Rectangular shapes with 1 mm in thickness were also cut for *in situ* electrical resistivity measurements from the same single crystal rod. The X-ray diffraction on single crystals surface was measured in texture analysis *Philips X'Pert* with CuKα radiation and Ni filter to determine the preferential orientation of the obtained samples. Figure 1 shows some pictures of sample preparation procedures.

2.2 In situ electrical resistivity measurements

Single crystals in rectangular blocks with the longest side parallel to the growth axis were used to study the kinetics of oxygen removal process by *in situ* electrical resistivity measurements.

For the electrical resistivity measurements, a sample holder was constructed with an alumina tube. Four platinum wires were connected to the sample with special epoxy, and the sample holder has a thermocouple with its tip installed near the specimen. The sample holder part is involved by a quartz tube and introduced inside of a heated stainless-steel enclosure continuously evacuated at 10^{-5} Torr by a turbo-mechanic vacuum pump. Software developed in *Matlab* programing language acquires the electrical resistance of the sample by standard four-probe method using *Keithley*
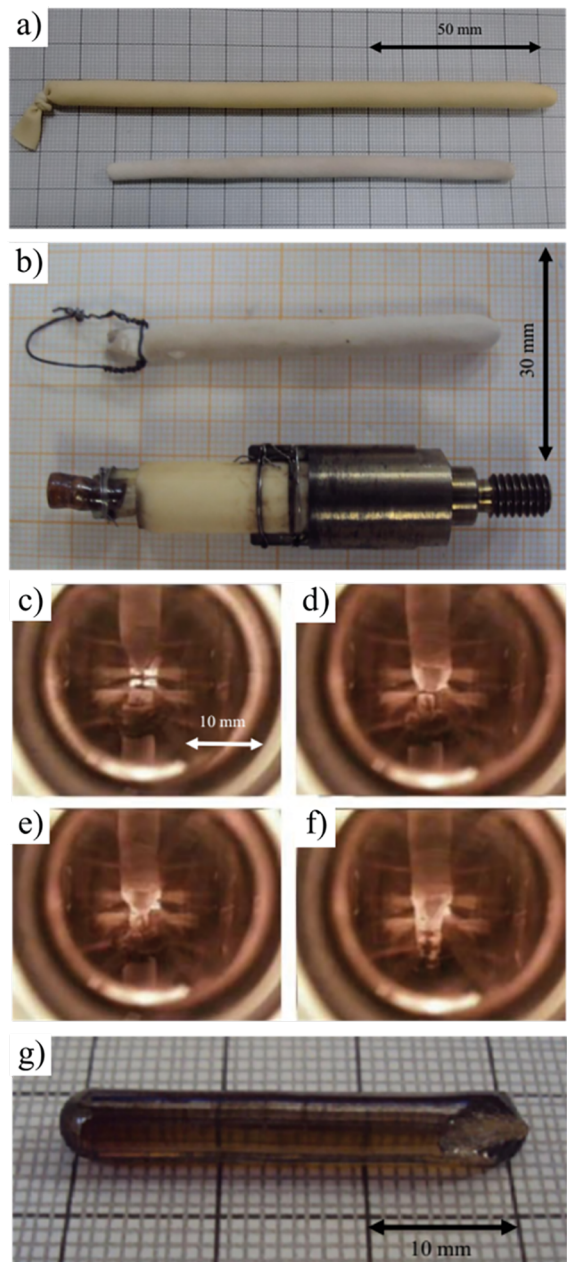

Figure 1. a) $SrTiO_3$ powder inside rubber mold (up) and $SrTiO_3$ feed rod after compressed and sintered (down). b) Single crystal as seed is connected to the Floating Zone furnace holder (up) and $SrTiO_3$ feed rood prepared for crystal growth process (down). In the pictures (c) to (f) one can see: c) feed rod (up) and seed (down) before feed rod melting; d) feed rod tip melted at hot zone; e) tip melted joined on the single-crystalline seed; and f) both feed rod and seed are pulling down with crystal growing below the hot zone. In (g) in shown a typical $SrTiO_3$ single crystal rod after the crystal growth.

2410 source meter and *Keithley Dmm-2000* multimeter controlled by *NI*-GPIB interface. Samples were excited with direct current of 10 µA in which characteristic I-V curves are in ohmic regime.

3. Results and Discussion

Figure 2 shows the X-ray diffraction (XRD) pattern for the SrTiO₃ polycrystalline powder and the structural refinement by GSAS program[27]. One can observe good agreement between experimental and refined patterns[28], which confirms SrTiO₃ single phase with lattice parameter a = 3.905 Å and Pm-3m space group[2,25]. The goodness refinement indices are: R_{exp} = 4.39%; R_p = 6.42%; R_{wp} = 7.76% and χ^2 = 3.12.
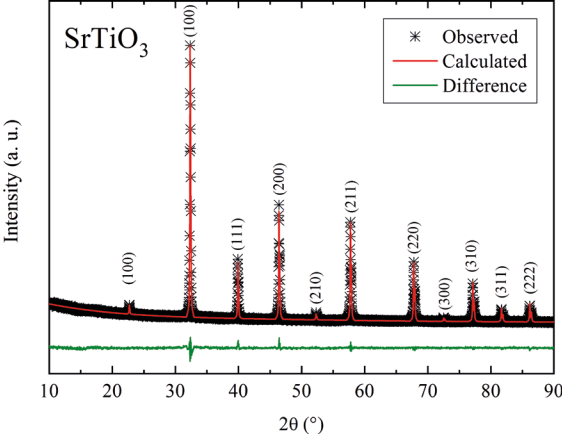
Figure 2. XRD pattern of SrTiO₃ powder synthetized by standard ceramic route.

The results of preferential orientation in single crystals are shown in Figure 3. Figure 3*a* shows that the surface on the disk shape samples has only diffraction patterns of the {100} family planes. This is an indicative of preferential growth axis parallel with [100] crystallographic orientation. On the other hand, one of the single crystals samples grew with [110] direction (see Figure 3*b*).

Figure 4 shows the evolution in electrical resistivity of a sample during thermal annealing at 650°C under a vacuum of 10^{-5} Torr. One can observe four regimes in Figure 4: *i*) a fast warming up to the temperature of the measurement, in which there is a decreasing of the electrical resistivity due to insulator behavior of the stoichiometric SrTiO₃; *ii*) a plateau up to 200 to 300 min depending on the annealing temperature; *iii*) a regime of stable temperature longer than 1200 minutes in which the oxygen removal occurs; and *iv*) a fast cooling down to room temperature. The behavior in the cooling regime indicates that under these experimental conditions used here, the amount of oxygen atoms removed from the samples was not high enough to produce metallic samples, such as reported before by other authors[29].

The equilibrium degree *α* during oxygen removal process at constant temperature regime can be written in terms of electrical conductivity by[18,20,21]:
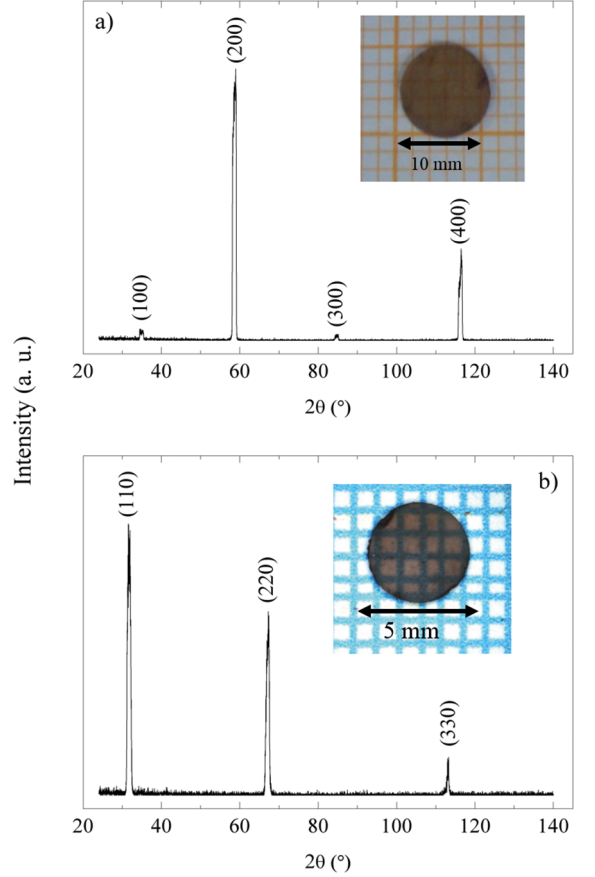
Figure 3. XRD of the single crystal surface with: a) [100] preferential orientation and b) [110] preferential orientation. The insets show the analyzed samples.

$$\alpha = \frac{\sigma - \sigma_0}{\sigma_\infty - \sigma_0}, \qquad (1)$$

where σ is electrical conductivity ($1/\rho$) at elapsed time t, σ_0 is the electrical conductivity at initial condition ($\alpha \approx 0$) and σ_∞ is the electrical conductivity when a new equilibrium is achieved ($\alpha \approx 1$).

In solid-state kinetic formalism, the evolution in the equilibrium degree can be expressed by a linear form allowed by some $g(\alpha)$ model-function[21]:

$$g(\alpha) = kt \qquad (2)$$

where the reaction rate constant k, is temperature dependent and given by:

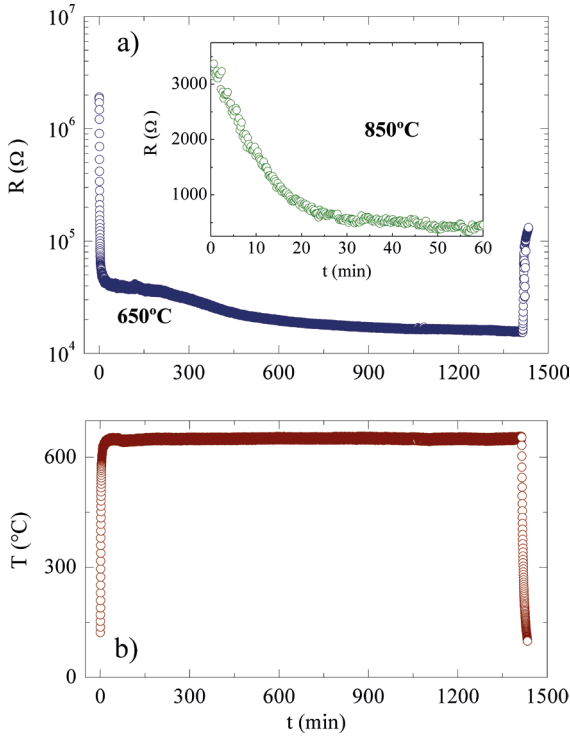$$k = A \exp\left(-\frac{E}{k_B T}\right), \qquad (3)$$

Figure 4. a) Evolution of the electrical resistivity of a SrTiO₃ single crystal as a function of time during annealing under vacuum of 10⁻⁵ Torr. In (b) is shown the temperature during the annealing. The Inset displays the acquired data at 850°C setting the initial time just after the plateau mentioned in the text.
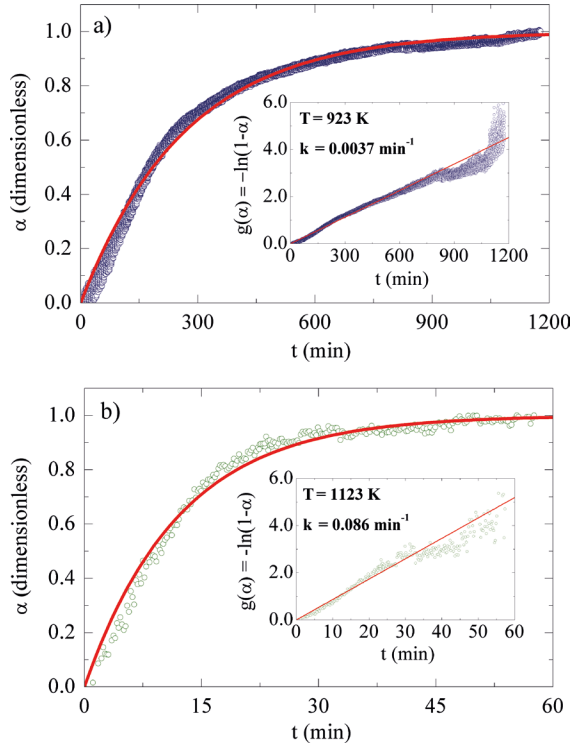

Figure 5. Equilibrium degree evolution calculated by equation (1) at isothermal temperatures of 650°C (a) and 850°C (b) under vacuum of 10⁻⁵ Torr. The initial time was set up at the starting point where the annealing temperature becomes stable, such as observed in Figure 4 (a). The insets show the linear model $- \ln (1 - \alpha) = kt$ due to the first-order kinetics for the oxygen removal process. The lines are the fitted models.

where A represents the frequency reaction factor, E is the activation energy of the process, k_B is the Boltzmann constant, and T is the absolute temperature. The first-order reaction model reviewed in reference[21] fits better our experimental data. It is implies:

$$g(\alpha) = - \ln(1 - \alpha), \qquad (4)$$

providing:

$$\alpha = 1 - e^{-kt}. \qquad (5)$$

The results for two equilibrium temperatures are shown in Figure 5. The solid lines show the best fit for the obtained data in this work.

From the fit of the function expressed by equation 5 or from the slope of lines shown in insets of the Figure 5 (a) and (b), one can obtain the Arrhenius kinetic factor (k) at the analyzed temperature. The values are (3.7 ± 0.7) 10^{-3} min⁻¹ and (8.6 ± 0.1) 10^{-2} min⁻¹ for 650°C and 850°C, respectively. In such way, the activation energy value for the charge doping through oxygen removal process in SrTiO₃ can be estimated as 1.4±0.3 eV using equation 3.

This activation energy is based upon the evolution of the equilibrium degree observed in the electrical resistivity during the annealing in vacuum at constant temperature, which can be related to possible three mechanisms: *i)* the formation of vacancies; *ii)* the oxygen self-diffusion; and *iii)* the oxygen desorption from the sample surface. A recently mechanism has been predicted theoretically in which easy diffusion path such as oxygen dislocations in SrTiO₃ has impact on resistive switch applications[30].

Within the standard deviation, our data is in good agreement with the recent value reported by Zhu *et al.* (1.0 eV), where a first-order kinetic model also fits their experimental data for *in situ* optical properties measurements[23].

Other similar energy values can be found on literature, however they are based upon oxygen diffusion models[18]. Some of these results are based upon similar electrical measurements reported here, but the authors attribute the influence on the electrical conductivity to the oxygen diffusion[18,20] or possible easy diffusion path such as oxygen dislocations[31] instead charge doping reaction as stressed out in this report.

4. Conclusions

In situ electrical resistivity measurements during reduction annealing under vacuum in $SrTiO_3$ single crystals grown by Floating Zone Method were well described by the general solid-state kinetics approach as a first-order mechanism providing information on the oxygen vacancies/charge doping formation. Additionally, this allowed us to determine the activation energy for the formation of oxygen vacancies as 1.4 ± 0.3 eV. This result is in good agreement with the data reported on literature within the experimental deviation.

5. Acknowledgements

6. References

1. Rice WD, Ambwani P, Bombeck M, Thompson JD, Haugstad G, Leigton C, et al. Persistent optically induced magnetism in oxygen-deficient strontium titanate. *Nature Materials*. 2014;13(5):481-487.

2. Zhang J, Xie K, Wei H, Qin Q, Qi W, Yang L, et al. In situ formation of oxygen vacancy in perovskite $Sr_{0.95}Ti_{0.8}Nb_{0.1}M_{0.1}O_3$ (M = Mn, Cr) toward efficient carbon dioxide electrolysis. *Scientific Reports*. 2014;4:7082.

3. Shang PP, Zhang BP, Liu Y, Li JF, Zhu HM. Preparation and Thermoelectric Properties of La-Doped $SrTiO_3$ Ceramics. *Journal of Electronic Materials*. 2011;40(5):926-931.

4. Trabelsi H, Bejar M, Dhahri E, Sajieddine M, Valente MA, Zaoui A. Effect of the oxygen deficiencies creation on the suppression of the diamagnetic behavior of $SrTiO_3$ compound. *Journal of Alloys and Compounds*. 2016;680:560-564.

5. de Lima BS, da Luz MS, Oliveira FS, Alves LMS, dos Santos CAM, Jomard F, et al. Interplay between antiferrodistortive, ferroelectric, and superconducting instabilities in $Sr_{1-x}Ca_xTiO_{3-\delta}$. *Physical Review B*. 2015;91(4):045108.

6. Zhong W, Vanderbilt D. Effect of quantum fluctuations on structural phase transitions in $SrTiO_3$ and $BaTiO_3$. *Physical Review B*. 1996;53(9):5047-5050.

7. Loetzsch R, Lübcke A, Uschmann I, Förster E, Große V, Thuerk M, et al. The cubic to tetragonal phase transition in $SrTiO_3$ single crystals near its surface under internal and external strains. *Applied Physics Letters*. 2010;96(7):071901.

8. Salje EKH, Gallardo MC, Jiménez J, Romero FJ, del Cerro J. The cubic-tetragonal phase transition in strontium titanate: excess specific heat measurements and evidence for a near-tricritical, mean field type transition mechanism. *Journal of Physics: Condensed Matter*. 1998;10(25):5535-5543.

9. Lin X, Bridoux G, Gourgout A, Seyfarth G, Krämer S, Nardone M, et al. Critical Doping for the Onset of a Two-Band Superconducting Ground State in $SrTiO_{3-\delta}$. *Physical Review Letters*. 2014;112(20):207002.

10. Koonce CS, Cohen ML, Schooley JF, Hosler WR, Pfeiffer ER. Superconducting Transition Temperatures of Semiconducting $SrTiO_3$. *Physical Review*. 1967;163(2):380-390.

11. Schooley JF, Hosler WR, Ambler E, Becker JH, Cohen ML, Koonce CS. Dependence of the Superconducting Transition Temperature on Carrier Concentration in Semiconducting $SrTiO_3$. *Physical Review Letters*. 1965;14(9):305-307.

12. Edge JM, Kedem Y, Aschauer U, Spaldin NA, Balatsky AV. Quantum Critical Origin of the Superconducting Dome in $SrTiO_3$. *Physical Review Letters*. 2015;115(24):247002.

13. Liu ZQ, Lü WM, Lim SL, Qiu XP, Bao NN, Motapothula M, et al. Reversible room-temperature ferromagnetism in Nb-doped $SrTiO_3$ single crystals. *Physical Review B*. 2013;87(22):220405.

14. Ohta S, Nomura T, Ohta H, Koumoto K. High-temperature carrier transport and thermoelectric properties of heavily La- or Nb-doped $SrTiO_3$ single crystals. *Journal of Applied Physics*. 2005;97(3):034106.

15. Yamada H, Miller GR. Point defects in reduced strontium titanate. *Journal of Solid State Chemistry*. 1973;6(1):169-177.

16. Balachandran U, Eror NG. Electrical conductivity in strontium titanate. *Journal of Solid State Chemistry*. 1981;39(15):351-359.

17. Szot K, Speier W, Carius R, Zastrow U, Beyer W. Localized Metallic Conductivity and Self-Healing during Thermal Reduction of $SrTiO_3$. *Physical Review Letters*. 2002;88(7):75508.

18. Pasierb P, Komornicki S, Rekas M. Comparison of the chemical diffusion of undoped and Nb-doped $SrTiO_3$. *Journal of Physics and Chemistry of Solids*. 1999;60(11):1835-1844.

19. Walters LC, Grace RE. Formation of point defects in strontium titanate. *Journal of Physics and Chemistry of Solids*. 1967;28(2):239-244.

20. Walters LC, Grace RE. Diffusion of point defects in strontium titanate. *Journal of Physics and Chemistry of Solids*. 1967;28(2):245-248.

21. Khawam A, Flanagan DR. Solid-State Kinetic Models: Basics and Mathematical Fundamentals. *Journal of Physics Chemistry B*. 2006;110(35):17315-17328.

22. Nabokin PI, Souptel D, Balbashov AM. Floating zone growth of high-quality $SrTiO_3$ single crystals. *Journal of the Crystal Growth*. 2003;250(3-4):397-404.

23. Zhu XD, Fei YY, Lu HB, Yang GZ. Role of step edges in oxygen vacancy transport into $SrTiO_3$(001). *Applied Physics Letters*. 2005;87(5):051903.

24. Koohpayeh SM, Fort D, Abell JS. The optical floating zone technique: A review of experimental procedures with special reference to oxides. *Progress in Crystal Growth and Characterization of Materials*. 2008;54(3-4):121-137.

25. Nassau K, Miller AE. Strontium titanate: An index to the literature on properties and the growth of single crystals. *Journal of the Crystal Growth*. 1988;91(3):373-381.

26. Guguschev G, Kok DJ, Galazka Z, Detlef KD, Uecker R, Bertram R, et al. Influence of oxygen partial pressure on $SrTiO_3$ bulk crystal growth from non-stoichiometric melts. *CrystEngComm*. 2015;17(17):3224-3234.

27. Toby BH. EXPGUI, a graphical user interface for GSAS. *Journal of Applied Crystallography*. 2001;34(Pt 2):210-213.

28. Toby BH. R factors in Rietveld analysis: How good is good enough? *Powder Diffraction*. 2006;21(1):67-70.

29. Spinelli A, Torija MA, Liu C, Jan C, Leighton C. Electronic transport in doped $SrTiO_3$: Conduction mechanisms and potential applications. *Physical Review B*. 2010;81(15):155110.

30. Szot K, Speier W, Bihlmayer G, Waser R. Switching the electrical resistance of individual dislocations in single-crystalline $SrTiO_3$. *Nature Materials*. 2006;5(4):312-320.

31. Marrocchelli D, Sun L, Yildiz B. Dislocations in $SrTiO_3$: Easy to Reduce but Not so Fast for Oxygen Transport. *Journal of the American Chemical Society*. 2015;137(14):4735-4748.